Photocurrent Estimation for a Self-Reset CMOS Image Sensor

Xinqiao Liu and Abbas El Gamal

Information Systems Laboratory
Department of Electrical Engineering
Stanford University
Stanford, CA 94305

chiao@stanford.edu, abbas@isl.stanford.edu

ABSTRACT

CMOS image sensors are capable of very high frame rate non-destructive readout. This capability and the potential of integrating memory and signal processing with the sensor on the same chip enable the implementation of many still and video imaging applications. An important example is dynamic range extension, where several images are captured during a normal exposure time — shorter exposure time images capture the brighter areas of the scene while longer exposure time images capture the darker areas of the scene. These images are then combined to form a high dynamic range image. Dynamic range is extended at the high end by detecting saturation, and at the low end using linear estimation algorithms that reduce read noise. With the need to reduce pixel size and integrate more functionality with the sensor, CMOS image sensors need to follow the CMOS technology scaling trend. Well capacity, however, decreases with technology scaling as pixel size and supply voltages are reduced. As a result, SNR decreases potentially to the point where even peak SNR is inadequate. In this paper, we propose a self-reset pixel architecture, which when combined with multiple non-destructive captures can increase peak SNR as well as enhance dynamic range. Under high illumination, self-resetting "recycles" the well during integration resulting in higher effective well capacity, and thus higher SNR. A recursive photocurrent estimation algorithm that takes into consideration the additional noise due to self-resetting is described. Simulation results demonstrate the SNR increase throughout the enhanced photocurrent range with 10dB increase in peak SNR using 32 captures.

Keywords: CMOS image sensor, self-reset, SNR, dynamic range, estimation

1. INTRODUCTION

CMOS image sensors are capable of very high frame rate non-destructive readout.[1–3] This capability when combined with the ability to integrate memory and signal processing with the sensor on the same chip can enable many new still and video imaging applications. An important example is dynamic range extension.[4,5,7] The idea is to capture several images at different times within a normal exposure time — shorter exposure time images capture the brighter areas of the scene while longer exposure time images capture the darker areas of the scene. The captured images are then combined into a single high dynamic range image by appropriately scaling each pixel's last sample before saturation. Conventional CDS is used to reduce reset and offset FPN. The scheme does not take full advantage of the multiple pixel samples, however. Readout noise, whose power is doubled as a result of performing CDS, remains as high as for conventional sensor operation. As a result dynamic range is only extended at the high illumination end. To more fully exploit the multiple pixel samples, we proposed a photocurrent estimation algorithm[7,8] that reduces read noise and thus enhances SNR and dynamic range at the low illumination end.

With the need to reduce pixel size and integrate more functionality with the sensor, CMOS image sensors continue to follow the CMOS technology scaling trend.[9] Well capacity, however, decreases with technology scaling. For a sensor operating in direct integration, well capacity can be expressed as

$$Q_{\text{well}} = V_{\text{swing}} \times C_{\text{sense}} \text{ Col.}$$

where V_{swing} is the voltage swing and C_{sense} is the integration capacitance. Both V_{swing} and C_{sense} decrease as technology scales. As a result, SNR decreases potentially to the point where even peak SNR ($\approx Q_{\text{well}}/q$) is inadequate.

In this paper, we propose a method for extending sensor peak SNR by combining a self-reset pixel architecture with multiple non-destructive image captures. Under high illumination, self resetting "recycles" the well during integration resulting in higher effective well capacity, and thus higher SNR. We extend our photocurrent estimation algorithm[7] to take into consideration the additional noise due to self-resetting.

The rest of the paper is organized as follows. In section 2 we describe the proposed self-reset pixel architecture. In section 3 we formulate the photocurrent estimation problem for the self-reset pixel architecture and present a recursive estimation algorithm. Finally, we present simulation results that demonstrate the dynamic range and SNR improvements using our algorithm.

2. SELF-RESET DIGITAL PIXEL SENSOR

The motivation for proposing the self-reset pixel architecture is to be able to increase the well capacity by reusing the small physical well several times during integration. Assuming a maximum of m self-resets, the well capacity becomes

$$Q_{\text{total}} = m \times Q_{\text{well}},$$

resulting in peak SNR of

$$\text{SNR}_{\text{peak}} \approx \frac{mQ_{\text{well}}}{q},$$

an m-fold increase in peak SNR.

The proposed self-reset pixel architecture is based on our latest Digital Pixel Sensor (DPS) design.[1] As shown in Figure 1, each pixel contains a photodiode, a comparator, a feedback loop and 8-bit memory. The design of the comparator and the memory has been described in.[1] The feedback loop consisting of transistors M1, M2, and M3 performs the self-reset function. The circuit has two modes of operation: multiple pixel sampling by means of A/D conversion and saturation monitoring. As shown in Figure 2, the operation alternates between these two modes during exposure.

During A/D conversion, which we assume to be performed at regular time interval, the V_{enable} signal is set low, and the feedback loop is off. Single-slope A/D conversion[1] is performed by ramping V_{ref} from V_{max} to V_{min} and digitally ramping *Bitline* from 0 to 255. The digital ramp is assumed to be generated by an on-chip counter and globally distributed to all pixels. The 8-bit memory cell latches the digital count corresponding to V_{in}'s value. The memory readout is performed during the following saturation monitoring mode.

During saturation monitoring, V_{enable} is high and V_{ref} is set at V_{min}. Light induced photocurrent discharges the diode capacitance and V_{in} continuously decrease till it reaches V_{min}, which causes the comparator to flip and its output V_1 to go high. This consequently turns on transistor M1 and V_2 goes low, which turns on M4 and resets the diode to V_{max}. After reset, V_1 becomes low again and M1 turns off. The very weakly biased transistor M3 gradually pulls up V_2 and finishes the self-reset.

Figure 3 shows HSPICE wave forms during self-resetting for the pixel circuit implemented in a standard 0.18μm CMOS technology using a comparator with gain bandwidth of 2.9GHz. Since self-resetting occurs asynchronously with A/D conversion, it may be interrupted by the A/D conversion before it is completed. Note that in our simulations the self-reset circuit loop delay is around 90ns and the ADC time is around 25μs. So, as long as the saturation monitoring period is much longer than 25μs, the probability of incomplete self-reset is quite low.

Note that self-resetting can be detected for a pixel provided that its photocurrent is constant during exposure time and the readout sampling rate is fast enough so that at least one sample is read out between every two consecutive self-resets. The multiple capture sampling rate, thus, sets an upper bound on the maximum detectable photocurrent.

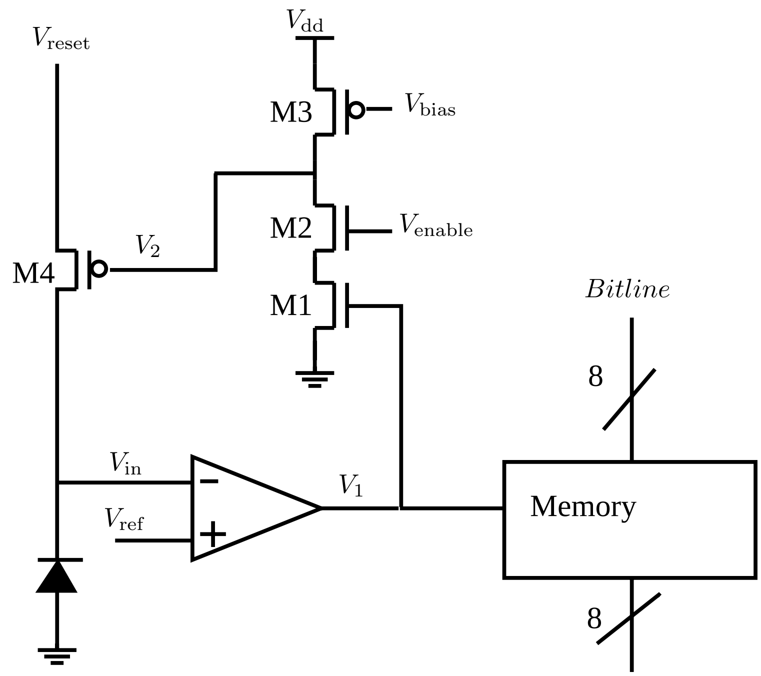

Figure 1. Self-reset Digital Pixel Sensor circuit.

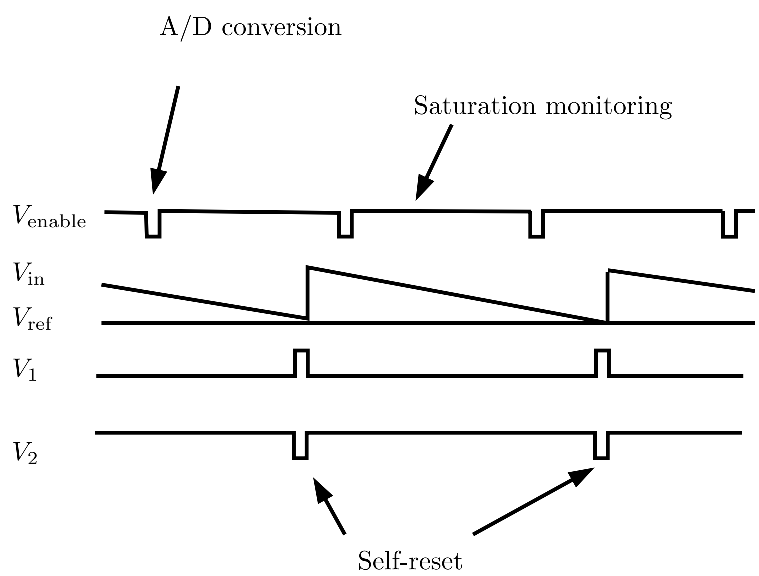

Figure 2. Self-reset Digital Pixel Sensor timing diagram.

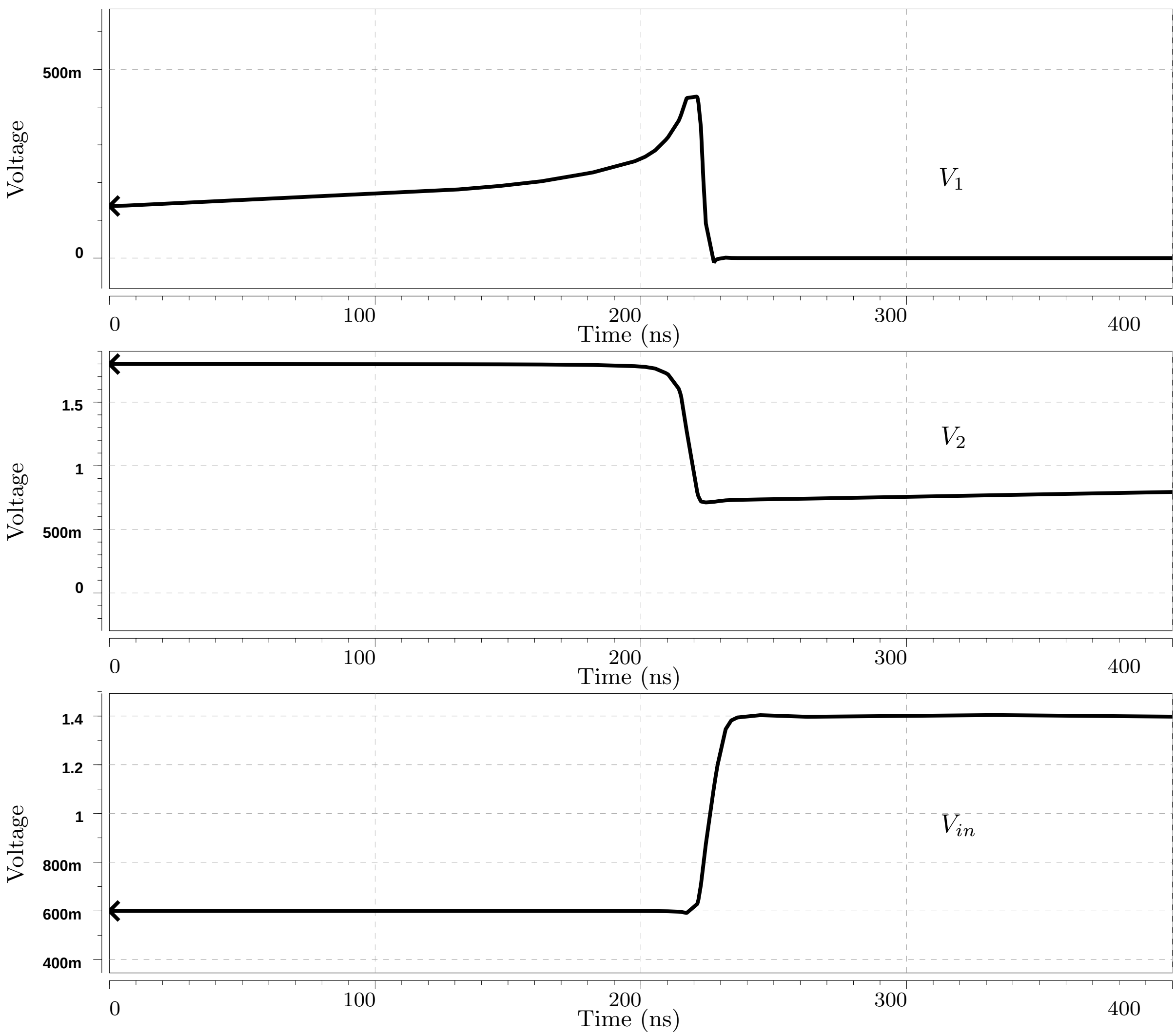

Figure 3. HSPICE wave forms of V_1, V_2 and V_{in} during self resetting for the pixel circuit implemented in a standard 0.18μm CMOS technology. The diode voltage V_{in} is reset from 0.6V to 1.4V in less than 90ns.

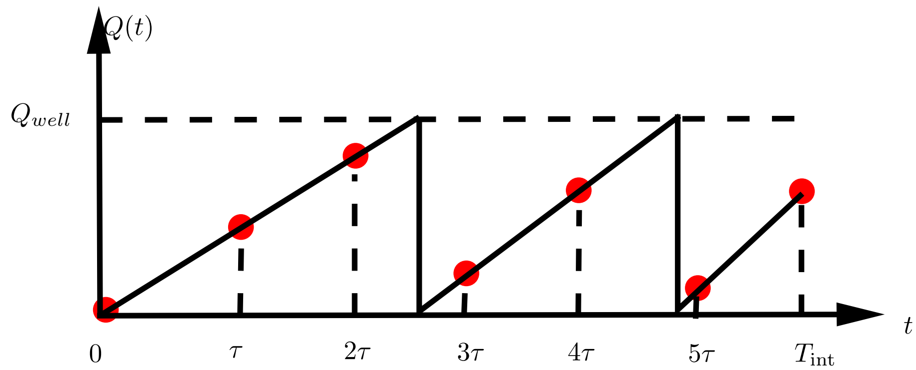

Figure 4. Photocharge as a function of time for the self-reset pixel where self-resetting happens twice during integration time $[0, T_{int}]$.

3. PHOTOCURRENT ESTIMATION ALGORITHM

In a previous paper,[7] we described a linear MSE estimation algorithm for estimating photocurrent from multiple pixel samples. In this section we modify the signal and noise model used in the previous paper and use it to derive a recursive estimation algorithm suited to the self-reset architecture.

Figure 4 provides an example of the integrated photocharge as a function of time for the self-reset pixel where self-resetting happens twice during integration time $[0, T_{int}]$. The image capture times, marked by the dashed lines, are uniformly spaced at time $t = 0, \tau, 2\tau, \ldots,$ and $T_{\rm int}$.

With the proposed self-reset scheme, reset noise and Fixed Pattern Noise (FPN) accumulate as self-resetting occurs. Assuming $n+1$ captures at times $0, \tau, \ldots, T_{\rm int}$, we denote the pixel charge sample at time $k\tau$ and after m self-resets by $Q_{k,m}$.

With the accumulated reset noise and FPN components taken into consideration, $Q_{k,m}$ is given by:

$$\begin{aligned} Q_{0,0} &= V_0 + G_0 + F, \text{ the initial sample,} \\ Q_{k,m} &= ik\tau + \sum_{j=1}^{k} U_j + V_k + \sum_{j=0}^{m} G_j + (m+1)F, \ 0 < k \leq n, \ 0 \leq m < k-1, \end{aligned}$$

where V_k is the readout noise of the kth sample, U_j is the shot noise generated during the time interval $((j-1)\tau, j\tau]$, G_j is the reset noise generated during the jth self-reset , and F is the offset FPN. The U_j, V_k, G_j, F are independent zero mean random variables with

$$\begin{aligned} E(V_k^2) &= \sigma_V^2 > 0, \text{ for } 0 \leq k \leq n, \\ E(U_j^2) &= \sigma_U^2 = qi\tau, \text{ for } 1 \leq j \leq k, \text{ and} \\ E(G_j^2) &= \sigma_G^2 > 0, \text{ for } 0 \leq j \leq m. \end{aligned}$$

We also assume that $F >> G_j$, *i.e.*, that FPN is much larger than reset noise, and thus performing CDS is close to optimal,[7] and define the photocurrent sample $\tilde{I}_k$ at time $k\tau$ as:

$$\begin{aligned} \tilde{I}_{k,m} &= \frac{Q_{k,m} - (m+1)Q_{0,0}}{k\tau} \\ &= i + \frac{1}{k\tau}\sum_{j=1}^{k} U_j + \frac{1}{k\tau}(V_k - (m+1)V_0) + \frac{1}{k\tau}(\sum_{j=1}^{m} G_j - mG_0), \text{ for } 1 \leq k \leq n. \end{aligned}$$

The photocurrent linear estimation problem can be formulated as follows:

Find the best unbiased linear mean square estimate of the parameter i given $\{\tilde{I}_{1,0}, \tilde{I}_{2,0}, \ldots, \tilde{I}_{n,m}\}$, i.e., *coefficients $a_1, a_2, \ldots, a_n$ such that*

$$\hat{I}_n = \sum_{j=1}^{n} a_j \tilde{I}_{j,m},$$

minimizes

$$\Phi_n^2 = E(\hat{I}_n - i)^2,$$

subject to

$$E(\hat{I}_n) = i.$$

In order to reduce the computational complexity and memory requirements of the estimation algorithm, we restrict ourselves to recursive estimates, *i.e.*, estimates that can be recursively updated after each sample. So the problem can be reformulated as:

At time $k\tau$, find

$$\hat{I}_k = \hat{I}_{k-1} + a_k(\tilde{I}_{k,m} - \hat{I}_{k-1}), \ \textit{for } 2 \le k \le n,$$

minimizes

$$\Phi_k^2 = E(\hat{I}_k - i)^2,$$

subject to

$$E(\hat{I}_k) = i.$$

The coefficient a_k can be found by solving the equations

$$\begin{aligned} \frac{d\,\Phi_k^2}{d\,a_k} &= \frac{d\,E(\hat{I}_k - i)^2}{d\,a_k} = 0, \text{ and} \\ E(\hat{I}_k) &= i. \end{aligned}$$

Define the MSE of $\tilde{I}_{k,m}$ as

$$\begin{aligned} \Delta_k^2 &= E(\tilde{I}_{k,m} - i)^2 \\ &= \frac{1}{k^2\tau^2}(k\sigma_U^2 + (m^2 + 2m + 2)\sigma_V^2 + (m^2 + m)\sigma_G^2), \end{aligned}$$

and the covariance between $\tilde{I}_{k,m}$ and $\hat{I}_k$ as

$$\begin{aligned} \Theta_k &= E(\tilde{I}_{k,m} - i)(\hat{I}_k - i) \\ &= (1 - a_k)E(\tilde{I}_{k,m} - i)(\hat{I}_{k-1} - i) + a_k\Delta_k^2. \end{aligned}$$

To derive the expression for Θ_k, we need to consider whether self-resetting has occurred before the current sample, *i.e.*, to represent $\tilde{I}_{k,m}$ using $\tilde{I}_{k-1,m}$ or $\tilde{I}_{k-1,m-1}$.

Thus we have:

$$\Theta_k = \begin{cases} (1 - a_k)\frac{k-1}{k}\Theta_{k-1} - \frac{(1-a_k)a_{k-1}}{k(k-1)\tau^2}\sigma_V^2 + a_k\Delta_k^2, & \text{for} \quad m \text{ self-resets} \\ (1 - a_k)\frac{k-1}{k}\Theta_{k-1} - \frac{(1-a_k)(m+a_{k-1})}{k(k-1)\tau^2}\sigma_V^2 + \frac{(1-a_k)(m-1)}{k(k-1)\tau^2}\sigma_G^2 + a_k\Delta_k^2, & \text{for} \quad m-1 \text{ self-resets.} \end{cases}$$

The MSE of $\hat{I}_k$ can be expressed in terms of Δ_k^2 and Θ_k as

$$\Phi_k^2 = (1-a_k)^2\Phi_{k-1}^2 + {a_k}^2\Delta_k^2 + 2(1-a_k)a_k\Psi_k,$$

where

$$\begin{aligned}
\Psi_k &= E(\hat{I}_{k-1}-i)(\tilde{I}_{k,m}-i) \\
&= \begin{cases} \frac{(k-1)}{k}\Theta_{k-1} - \frac{a_{k-1}}{k(k-1)\tau^2}\sigma_V^2 & \text{for} \quad m \text{ self-resets} \\ \frac{(k-1)}{k}\Theta_{k-1} - \frac{(m+a_{k-1})}{k(k-1)\tau^2}\sigma_V^2 - \frac{(m-1)}{k(k-1)\tau^2}\sigma_G^2 & \text{for} \quad m-1 \text{ self-resets.} \end{cases}
\end{aligned}$$

To minimize the MSE, we require that

$$\frac{d\,\Phi_k^2}{d\,a_k} = 0,$$

which gives

$$a_k = \frac{\Phi_{k-1}^2 - \Psi_k}{\Phi_{k-1}^2 + \Delta_k^2 - 2\Psi_k}.$$

Note that a_k, Θ_k and Ψ_k can all be recursively updated.

To summarize, the recursive algorithm is as follows.

Compute initial parameter values:

$$\begin{aligned}
a_1 &= 1, \\
\tilde{I}_{1,0} &= \frac{(Q_1-Q_0)}{\tau}, \\
\hat{I}_1 &= \tilde{I}_1, \\
\Delta_1^2 &= \frac{\sigma_U^2 + 2\sigma_V^2}{\tau^2}, \\
\Phi_1^2 &= \Delta_1^2, \\
\Theta_1 &= \Delta_1^2.
\end{aligned}$$

At each iteration, update the parameter values:

$$\begin{aligned}
\tilde{I}_{k,m} &= \frac{Q_{k,m} - (m+1)Q_{0,0}}{k\tau}, \\
\Delta_k^2 &= \frac{1}{k^2\tau^2}(k\sigma_U^2 + (m^2+2m+2)\sigma_V^2 + (m^2+m)\sigma_G^2), \\
\Psi_k &= \begin{cases} \frac{(k-1)}{k}\Theta_{k-1} - \frac{a_{k-1}}{k(k-1)\tau^2}\sigma_V^2 & \text{for} \quad m \text{ self-resets} \\ \frac{(k-1)}{k}\Theta_{k-1} - \frac{(m+a_{k-1})}{k(k-1)\tau^2}\sigma_V^2 - \frac{(m-1)}{k(k-1)\tau^2}\sigma_G^2 & \text{for} \quad m-1 \text{ self-resets} \end{cases} \\
a_k &= \frac{\Phi_{k-1}^2 - \Psi_k}{\Phi_{k-1}^2 + \Delta_k^2 - 2\Psi_k}, \\
\Theta_k &= \begin{cases} (1-a_k)\frac{k-1}{k}\Theta_{k-1} - \frac{(1-a_k)a_{k-1}}{k(k-1)\tau^2}\sigma_V^2 + a_k\Delta_k^2 & \text{for} \quad m \text{ self-resets} \\ (1-a_k)\frac{k-1}{k}\Theta_{k-1} - \frac{(1-a_k)(m+a_{k-1})}{k(k-1)\tau^2}\sigma_V^2 + \frac{(1-a_k)(m-1)}{k(k-1)\tau^2}\sigma_G^2 + a_k\Delta_k^2 & \text{for} \quad m-1 \text{ self-resets} \end{cases} \\
\Phi_k^2 &= (1-a_k)^2\Phi_{k-1}^2 + {a_k}^2\Delta_k^2 + 2(1-a_k)a_k\Psi_k, \\
\hat{I}_k &= \hat{I}_{k-1} + a_k(\tilde{I}_{k,m} - \hat{I}_{k-1}).
\end{aligned}$$

Note that to find the new estimate $\hat{I}_k$, only three parameters, a_k, Φ_k and Θ_k, the old estimate $\hat{I}_{k-1}$ and the new sample value $\tilde{I}_{k,m}$ are needed. Thus only a small fixed amount of memory per pixel independent of the number of captures is required.

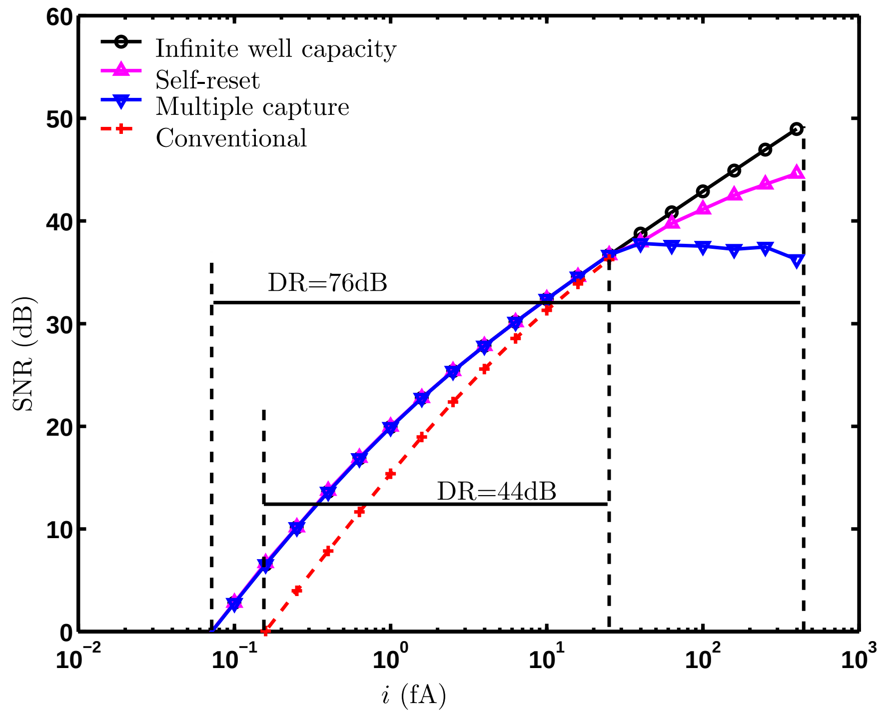

Figure 5. SNR and dynamic range comparison with well capacity $Q_{\text{well}} = 6250e^{-}$, readout noise of $30e^{-}$, reset noise of $8e^{-}$ and total 32 multiple captures. The circled line is a sensor with infinite well capacity serving as a theoretical upper bound.

Figure 5 compares SNR for a conventional sensor, a sensor using multiple capture and MSE estimation, and a self-reset sensor. The conventional sensor has dynamic range of 44dB and peak SNR of 36dB. Using linear estimation and saturation detection[7] dynamic range is extended to 76dB — 8dB gain at the low illumination end and 24dB at the high illumination end. SNR is enhanced at low illumination but peak SNR remains the same. Now, using the proposed self-reset pixel architecture and in combination with the modified estimation algorithm, we can achieve the 76dB dynamic range, enhance SNR at the low illumination end, as well enhance peak SNR by 10dB. Note that the enhanced SNR is very close to the theoretical (and un-achievable) upper bound of 50dB for a sensor with infinite well capacity. The difference in SNR is due to the accumulation of reset noise due to the multiple resets.

4. CONCLUSION

CMOS image sensors can benefit from technology scaling by reducing pixel size, increasing fill factor, reducing power consumption, and integrating more functionality on the same chip. However, sensor SNR deteriorates as technology scales due to the reduction in well capacity. The paper described a self-reset DPS architecture that solves this problem by reusing the well several times during exposure time. The sensor is read out multiple times during exposure to detect the self-resets. We described a recursive estimation algorithm that uses the multiple capture to further enhance SNR by reducing the accumulated reset and readout noise. Simulation results using self-resetting and recursive estimation demonstrated enhanced peak SNR that is close to the ideal case of unbounded well capacity.

The self-reset architecture we described has several other side benefits including: (i) the possibility of further reduction in pixel size and fill factor since large well capacity is no longer necessary, (ii) more relaxed ADC design requirements due to the large effective signal swing, and (iii) eliminating the need for an anti-blooming device in each pixel.

5. ACKNOWLEDGMENTS

The work reported in the paper is supported under the Programmable Digital Camera Program by Agilent, Canon, HP, Interval Research and Kodak. The authors wish to thank Professor Brian Wandell and Ting Chen, SukHwan Lim, Khaled Salama and Helmy Eltoukhy for helpful discussions.

REFERENCES

1. S. Kleinfelder, S.H. Lim, X. Liu, and A. El Gamal, "A 10,000 frames/s 0.18 um CMOS digital pixel sensor with pixel-level memory", 2001 IEEE International Solid State Circuit Conference, Digest of Technical Papers, San Francisco, Feb 2001.
2. A. Krymski, D. Van Blerkom, A. Andersson, N. Block, B. Mansoorian and E. R. Fossum, "A High Speed, 500 Frames/s, 1024×1024 CMOS Active Pixel Sensor", in *Proceedings of the 1999 Symposium on VLSI Circuits*, pp. 137-138, Jun. 1999.
3. N. Stevanovic, M. Hillegrand, B. J. Hostica and A. Teuner, "A CMOS Image Sensor for High Speed Imaging", in *Proceedings of the 2000 IEEE International Solid-State Circuits Conference*, pp. 104-105, Feb. 2000.
4. O. Yadid-Pecht and E. Fossum, "Wide intrascene dynamic range CMOS APS using dual sampling," *IEEE Trans. on Electron Devices*, Vol. 44 No. 10, pp. 1721-1723, Oct. 1997.
5. D. Yang, A. El Gamal, B. Fowler, and H. Tian, "A 640x512 CMOS image sensor with ultra-wide dynamic range floating-point pixel level ADC", *IEEE J. Solid-State Circuits*, Vol.34, no.12, pp. 1821-1834, Dec. 1999.
6. D.Yang and A. El Gamal, "Comparative Analysis of SNR for Image Sensors with Enhanced Dynamic Range", *Proceedings of the SPIE*, Vol. 3649, San Jose, CA, January 1999.
7. X. Liu and A. El Gamal, "Photocurrent estimation from multiple non-destructive samples in a CMOS image sensor", Proceeding of SPIE, Vol. 4306, San Jose, March, 2001.
8. X. Liu and A. El Gamal, "Simultaneous Image Formation and Motion Blur Restoration via Multiple Capture", Proceeding of International Conference on Acoustic, Speech and Signal Processing, Salt Lake City, May, 2001.
9. H. Wong, "Technology and Device Scaling Considerations for CMOS Imagers", *IEEE Trans. on Electron Devices*, Vol 43. No 12. pp.2131-2142, Dec. 1996.